The Journal of Adhesion, 85:512–525, 2009

ISSN: 0021-8464 print/1545-5823 online
DOI: 10.1080/00218460902996390

Taylor & Francis
Taylor & Francis Group

The Crowding Model as a Tool to Understand and Fabricate Gecko-Inspired Dry Adhesives

Noshir S. Pesika[1], Nick Gravish[2], Matt Wilkinson[2], Boxin Zhao[3], Hongbo Zeng[4], Yu Tian[5], Jacob Israelachvili[4], and Kellar Autumn[2]

[1]Chemical and Biomolecular Engineering Department, Tulane University, LA, USA
[2]Department of Biology, Lewis and Clark College, Portland, OR, USA
[3]Chemical Engineering Department, University of Waterloo, Ontario, Canada
[4]Chemical Engineering Department, University of California, Santa Barbara, CA
[5]State Key Laboratory of Tribology, Department of Precision Instruments, Tsinghua University, Beijing, China

A model based on geometrical considerations of pillars in a square lattice is analyzed to predict its compression behavior under an applied normal load. Specifically, the "crowding model" analyzes the point at which tilting pillars become crowded onto neighboring pillars, which limits the achievable tilt angle under an applied normal load, which in turn limits their adhesion and friction forces. The crowding model is applied to the setal arrays of the tokay gecko. Good agreement is found between the predictions of the crowding model (a critical tilt angle of $\theta_c = 12.6^\circ$ *to the substrate corresponding to a vertical compression of* $\Delta z = 49\,\mu m$ *of the setae within the setal array) and experimental data for the compression of tokay gecko setal arrays. The model is also used as a criterion to predict the number density of setae in a tokay gecko setal array based on the lateral inter-pillar spacing distance, s, between tetrads of setae and the effective diameter, d, of the tetrad. The model predicts a packing density of* $\sim 14{,}200\,setae/mm^2$, *which is again in good agreement with the measured value of* $\sim 14{,}400\,setae/mm^2$. *The crowding model can be used as a tool to determine the optimum geometrical parameters, including the diameter and the spacing distance between pillars, to fabricate dry adhesives inspired by the gecko.*

Received 11 December 2008; in final form 12 March 2009.

One of a Collection of papers honoring J. Herbert Waite, the recipient in February 2009 of *The Adhesion Society Award for Excellence in Adhesion Science, Sponsored by 3M.*

Address correspondence to Kellar Autumn, Department of Biology, Lewis and Clark College, Portland, OR 97219, USA. E-mail: autumn@lclark.edu

Keywords: Adhesion; Bio-inspired adhesives; Crowding model; Dry adhesives; Friction; Gecko

INTRODUCTION

The gecko adhesive system is composed of densely packed fibrillar structures ranging from the macroscale to the nanoscale ordered into hierarchical levels [1,2]. The adhesive's structural complexity enables strong, controllable friction and adhesion [3,4]; however, research is still underway to understand the specific contributions from each of the many hierarchical levels [5–9]. The fact that van der Waals forces are responsible for gecko adhesion [10] has motivated the fabrication of gecko-inspired synthetic dry adhesives [11–13], which in turn requires a detailed understanding of the design parameters of the gecko system.

One of the key features of the gecko adhesive system is the fact that it allows for intimate contact of the spatula pads to surfaces of different roughness [14–16], which is attributed to the high level of compliance (*i.e.*, the ability of the gecko adhesive system to conform to the topology of a surface) provided by the different hierarchical structures [17]. As shown in Fig. 1, the tokay gecko (*Gekko gecko*) setal array consists of hair-like outgrowths called setae, which provide an intermediate level of compliance to the adhesive. The setae are, on average, 100 μm in length and 2.1 μm in radius, and tilted at 45° (see Fig. 2) when unstressed or at rest. They are densely packed in a square lattice in groups of four (tetrads) on the underside of the gecko's toes [1,2,18]. The setae are made of β-keratin, which has a relatively high Young's modulus of approximately 1.4 GPa [19]; however, under small compressive deformations the fibrils bend, resulting in a greatly reduced overall or effective Young's modulus (E_{eff}) of approximately 100 kPa [17].

To adhere, tokay gecko setae must achieve a seta-substrate angle, hereafter referred to as the tilt angle, of less than $\theta = 30°$ [3,20], which also results in a low spatula-substrate angle to allow for the strong friction required for enhancing the adhesion [6]. However, as the seta-substrate angle is decreased from its rest position during compressive strains, setal mobility is reduced once the setae begin to touch neighboring setae, thus, limiting the achievable tilt angle.

In this paper we derive a general model to explain the compression behavior of cylindrical pillars ordered in a square lattice (similar to tokay gecko setal arrays) based on the relevant geometrical

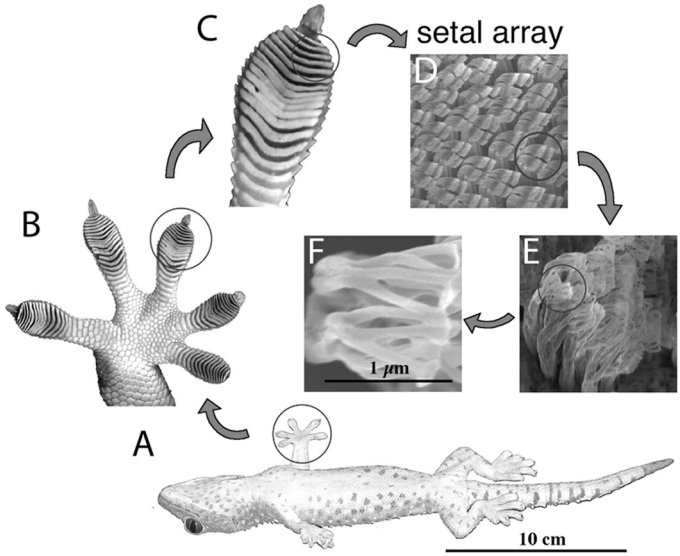

FIGURE 1 Hierarchical structures of the tokay gecko. Optical image showing (A) an inverted gecko at rest, (B) a gecko foot, and (C) a gecko toe. Scanning electron microscope images of (D) a setal array, (E) the spatula pads, and (F) a magnified view of the spatulae pads. Reprinted with permission from [5]. © 2006, National Academy of Sciences, USA.

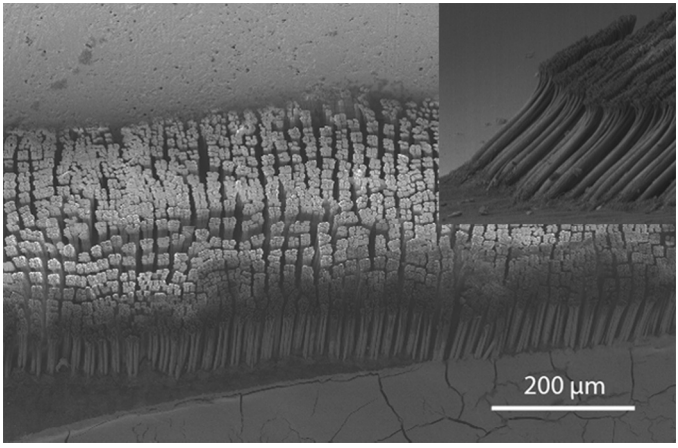

FIGURE 2 Scanning electron microscope image showing the top view of a setal array with setae packed as tetrads in a square lattice configuration. The inset shows a side view of the unstressed setal array with the setae naturally tilted at $\theta_o = 45^\circ$.

parameters of the system; these are shown in Fig. 3 and include the diameter, d, and length, L, of the pillars, the inter-pillar spacing, $s = s_x = s_y$, and the unstressed height, z_o, and tilt angle, θ_o, of the pillars. The model determines the point at which, upon further compression, pillars "crowd" onto each other, limiting the lowest achievable critical tilt angle, θ_c. It has previously been shown [5,6] that the adhesion and friction forces of gecko setal arrays increase as θ decreases based on the peel zone model [6]. Therefore, θ_c limits the maximum achievable adhesion force in the gecko adhesive system. The crowding model is also used to predict the compressive behavior of tokay gecko setal arrays when subjected to high compressive strains ($\sim$85%). In addition, the model is used as a criterion to predict the number density of setae in a tokay gecko setal array based on the lateral inter-pillar spacing distance, s, between tetrads of setae and the effective diameter, d, of the tetrad. The "crowding model" provides a guide for the design of gecko-inspired synthetic adhesives.

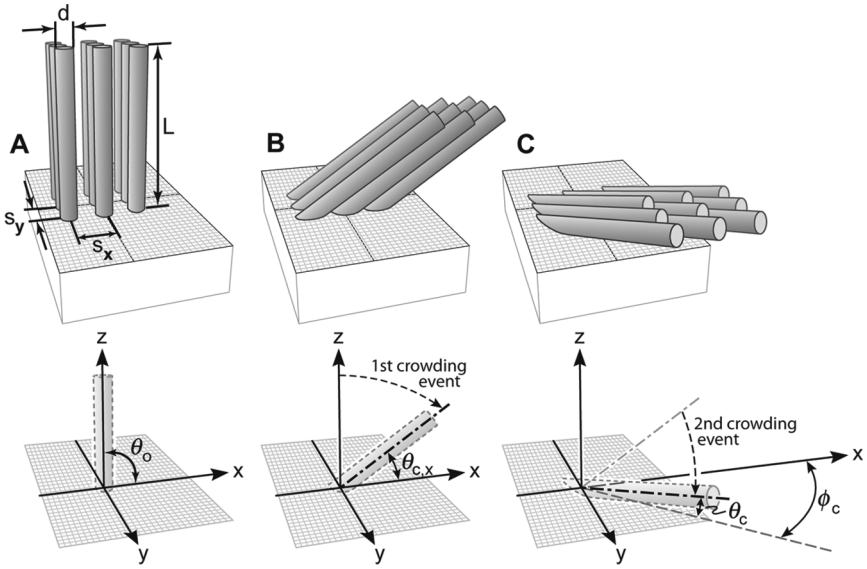

FIGURE 3 Schematic illustration of a square array of pillars of length L, with inter-pillar spacing s_x and s_y, subjected to a compressive force. (A) Unstressed pillars initially at rest with an angle θ_o with respect to the x-y plane. (B) Pillars experiencing a first crowding event causing them to crowd in the x-axis at a critical angle $\theta_{c,x}$. (C) Pillars experiencing a second, and final crowding event in the y-axis upon further compression resulting in a critical angle θ_c.

EXPERIMENTAL

Sample Preparation and Testing

Setal array samples were collected and prepared, and force measurements were made using a RoboToe system in the Autumn lab as previously described [21]. Arrays were gathered from live non-molting Tokay geckos (*Gekko gecko*). The average area of the 13 arrays used was $6.8 \times 10^{-7}\,m^2$ with a standard deviation of $2.8 \times 10^{7}\,m^2$. Excess skin was trimmed from each array using a dissection microscope. Setal arrays were then mounted to scanning electron microscope stubs using Loctite® 410 (Henkel Co., Rocky Hill, CT, USA). Prior to mechanical testing, samples were inspected to ensure no wicking of glue occurred in the setal shafts, and pictures were taken for area measurements.

Vertical load-pull testing of setal arrays was conducted to examine the compressive force, F, during an applied normal displacement, Δz, from the unstressed height of the setal array, z_o. Load-pull tests were performed using Teflon®-coated glass slides to compress the setal arrays by 60 μm or equivalent to approximately 85% strain. The unstressed height, z_o, of the setal array is ~70 μm based on the initial tilt angle, $\theta_o = 45^\circ$, and average length, $L = 100$ μm, of the setae. Samples were loaded and unloaded at a rate of 500 μm/s. The modulus of samples, E, was calculated for the first 20 μm and last 5 μm of the loading cycle and scaled to the area of the setal array, A, using $E = \frac{\Delta F \cdot z_o}{A \cdot \Delta z}$, where ΔF was the force change over the displacement Δz.

Adhesion and friction forces were measured using load-drag-pull tests. Load motions were performed at 45° to the test substrate so that setal arrays were pulled in shear during preloading. Setal arrays were dragged for 1 mm at 500 μm/s and friction and adhesion forces were calculated by averaging the steady state forces. Pull motions were performed at 135° to the test substrate, also causing setae to be dragged in shear during detachment.

Glass and Teflon-coated (Ted Pella, Redding, CA, USA) microscope slides were used as testing substrates for all tests. Glass slides were soaked in 2 M NaOH (Ted Pella, Redding) for 10 min prior to testing and then rinsed with DI water. Teflon®-coated slides were rinsed in DI water and wiped dry with Kimwipes® (Kimberly-Clark, Neenah, WI, USA). All experiments were conducted under ambient conditions.

RESULTS AND DISCUSSION

During the compression of pillars as shown in Fig. 3, we assume that the pillars behave as rigid beams and bend at their base until they

crowd or come in contact with their neighbors. The latter assumption is based on visual observations in the Autumn laboratory, where it was found that the setae bend predominantly at their base. During the initial compression, the bending of the beams allows for a significantly lower effective Young's modulus, E_{eff}. Upon further compression, the pillars approach their maximum packing density and behave as a solid material. The effective modulus, E_{eff}, of the crowded structure is now more representative of the bulk compressive modulus of the material, which in the case of the gecko would be β-keratin. A model, hereafter referred to as the crowding model, is derived based on the above assumptions and uses the experimentally determined geometrical parameters (these include the diameter, d, and length, L, of the pillars, the inter-pillar spacing, s_x and s_y, and the unstressed height, z_o, and tilt angle, θ_o, of the pillars) from SEM images of setal arrays of a tokay gecko to predict the point at which the setal array attains maximum crowding (*i.e.*, the critical compression depth, Δz_c, and the minimum achievable tilt angle or the critical angle, θ_c).

By modeling individual setae as rigid beams with length L (where $L > s$) that tilt about their base, the crowding criterion for setae along a single axis with diameter, d, and column spacing, s_x and s_y is

$$\sin(\theta_{c,x}) = \frac{d}{s_x} \quad \text{and} \quad \sin(\theta_{c,y}) = \frac{d}{s_y}, \tag{1}$$

where $\theta_{c,x}$ and $\theta_{c,y}$ are the crowding angles along a single axis. The latter represent the *first* possible crowding event as a result of the pillars getting in contact with their closest neighbors in the array. The pillars can further tilt into the perpendicular axis to form a close packed array of pillars. At the final crowding point, the tilt angle of the beams is given by

$$\theta_c = \sin^{-1}\left[\sin\theta_{c,x}\sin\theta_{c,y}\right], \tag{2}$$

and the beams are oriented with respect to the x-axis at an angle ϕ_c (or the azimuthal angle) given by

$$\phi_c = \tan^{-1}\left[\tan\theta_{c,x}\cos\theta_{c,y}\right]. \tag{3}$$

In the case of the tokay gecko, since the setae group as tetrads, the diameter of the beam structures, d, is approximately equal to four times the radius of individual setae (*i.e.*, $d = 4r = 8.4\,\mu\text{m}$). Also, since the setae are aligned in a square grid, the inter-pillar spacing $s_x = s_y = s = 18\,\mu\text{m}$. From Eq. (1), we obtain $\theta_{c,x} = \theta_{c,y} = 27.8^\circ$ and the critical angle reduces to

$$\theta_c = \sin^{-1}\left[\sin^2\theta_{c,x}\right] = 12.6^\circ, \tag{4}$$

with the beams oriented with respect to the x-axis at

$$\phi_c = \tan^{-1}\left[\sin\theta_{c,x}\right] = 25.0^\circ. \tag{5}$$

Figure 4a shows a plot of the compressive force, F, as a function of the vertical displacement, Δz, during a loading and unloading cycle. During compression, Δz is related to the change in the tilt angle, θ, of the seta as follows:

$$\theta = \sin^{-1}\left(\frac{L\sin\theta_o - \Delta z}{L}\right) \tag{6a}$$

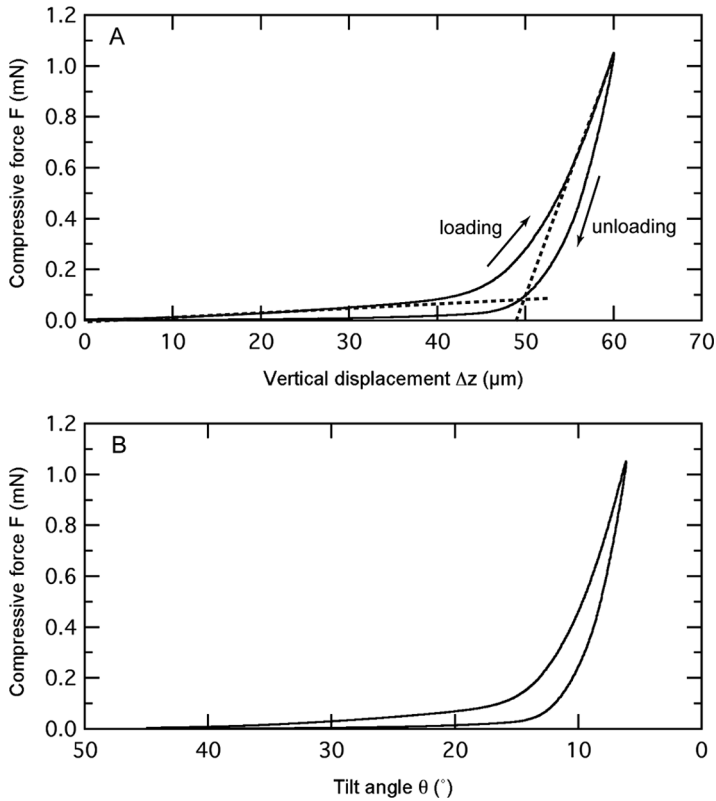

FIGURE 4 Plot of the force F experienced by the setal array during compression against a Teflon-coated glass slide at a rate of 500 μm/s expressed as a function of (A) the distance Δz and (B) the tilt angle θ given by Eq. (6a). The average area of the setal array $A = 6.8 \times 10^{-7}\,\mathrm{m}^2$.

or

$$\Delta z = L(\sin\theta_o - \sin\theta), \tag{6b}$$

where θ_o is the initial or unstressed tilt angle of the setae (*i.e.*, in the absence of load). Figure 4b shows the same data as Fig. 4a re-plotted as a function of the tilt angle, θ, as determined by Eq. (6a). According to Eq. (4), the angle at which the final crowding event occurs is 12.6° or equivalent to a vertical critical displacement, Δz_c, of 49 μm (using $L = 100\,\mu\text{m}$, $\theta_o = 45°$, and $\theta_c = 12.6°$ in Eq. (6b). The predicted values for the final crowding event are in good agreement with the experimental data. During the initial compression, an almost linear regime with a relatively low compression modulus (~129 KPa, using an average area of the setal arrays of $A = 6.8 \times 10^{-7}\,\text{m}^2$) is obtained until a vertical displacement of approximately 24 μm, corresponding to the first crowding event where $\theta_{c,x} = 27.8°$, at which point the compressive force enters a transition regime. We note that during the initial compression regime, an increasing fraction of setae contribute to the compressive force because of the non-uniformity in the heights of the setae. In the transition regime, the compressive force increases rapidly as the setae begin to crowd more densely until the setae approach the critical crowding angle $\theta_c = 12.6°$ and oriented at $\phi_c = 25.0°$. At this point, corresponding to a vertical displacement, Δz, of 49 μm, a second almost linear regime is achieved of much higher modulus (~3.0 MPa, using an average area of the setal arrays of $A = 6.8 \times 10^{-7}\,\text{m}^2$). Since the setae are porous structures and the setal array can deform further through lateral sliding of the setae to fill in interstitial gaps, we do not expect the higher modulus measured to be that of β-keratin but rather an effective modulus of the crowded structure.

The crowding model assumes that the pillars are identical and crowding events occur instantaneously. However, the gecko setal array consists of setae with a small variance in the setae length and tilt angle [22] which results in a less abrupt change in the compressive force from the un-crowded to crowded state (*i.e.*, during the compression of a setal array, an increasing number of setae contribute to the compressive force as the setae enter the crowded state). We can employ a logistic model [23] to predict the compressive force, F, of a setal array as an increasing fraction of setae transitions to the crowded state during further compression. Uncrowded setae exhibit a low normal stiffness, $k_{uncrowded}$, associated with bending of the setal shafts while crowded setae exhibit a much larger stiffness, $k_{crowded}$, as a result of setae in contact with neighboring setae. Assuming that the setal array behaves elastically under a normal compression (z), the force, $F_{uncrowded}$, generated by the bending of the uncrowded

setae is

$$F_{uncrowded} = k_{uncrowded} z, \tag{7a}$$

while the force generated by the crowded setae $F_{crowded}$ is

$$F_{crowded} = k_{crowded} z - F_{\mathrm{o}}, \tag{7b}$$

where F_{o} is a fitting constant to account for the fact that the setae do not crowd immediately upon compression.

Therefore, for a given fraction of setae in the uncrowded state $N_{uncrowded}$ and the remaining setae in the crowded state $N_{crowded}$ (*i.e.*, $N_{uncrowded} + N_{crowed} = 1$), the total compressive force, $F(z)$, exerted by the setal array under compressive strain is given by

$$F(z) = [N_{uncrowded} F_{uncrowded}] + [N_{crowded} F_{crowded}]. \tag{8}$$

Using a simple logistic growth differential equation to model the transition from the uncrowded state to the crowded state, the fraction of crowded setae can be expressed as

$$\frac{dN_{crowded}}{dz} = N_{crowded}(1 - N_{crowded}). \tag{9}$$

Substituting the solution to Eq. (9) into Eq. (8), the general solution to the compressive force during the crowding of the setae in the setal array is

$$\begin{aligned} F(z) = &\left[(k_{uncrowded} z)\left(1 - \frac{1}{1 + e^{-(z - z_{crowd})/u}}\right)\right] \\ &+ \left[(k_{crowded} z - F_{\circ})\left(\frac{1}{1 + e^{-(z - z_{crowd})/u}}\right)\right] \end{aligned} \tag{10}$$

where z_{crowd} is the displacement at which point half of the setae are in the crowded state (or $N_{crowded} = N_{uncrowded} = 0.5$), and u is the displacement over which the setae transition from an uncrowded state to a crowded state under incremental compressive loading. Fitting Eq. (10) to the force-displacement data in Fig. 4a results in fit parameters of $k_{uncrowded} = 1.57\,\mathrm{N/mm}$, $k_{crowded} = 51.1\,\mathrm{N/mm}$, $z_{crowd} = 58\,\mu\mathrm{m}$, $u = 5\,\mu\mathrm{m}$, and $F_o = 1.36\,\mathrm{N}$. These results predict that the crowding of the setae begins at approximately $\Delta z = z_{crowd} - \mathrm{u} = 53\,\mu\mathrm{m}$, which is reasonably consistent with the value of $\Delta z_c = 49\,\mu\mathrm{m}$ according to Eq. (6b).

In addition to using the crowding model to analyze the point at which crowding events occur, the model also provides a powerful predictive model to determine the maximum number density of angled

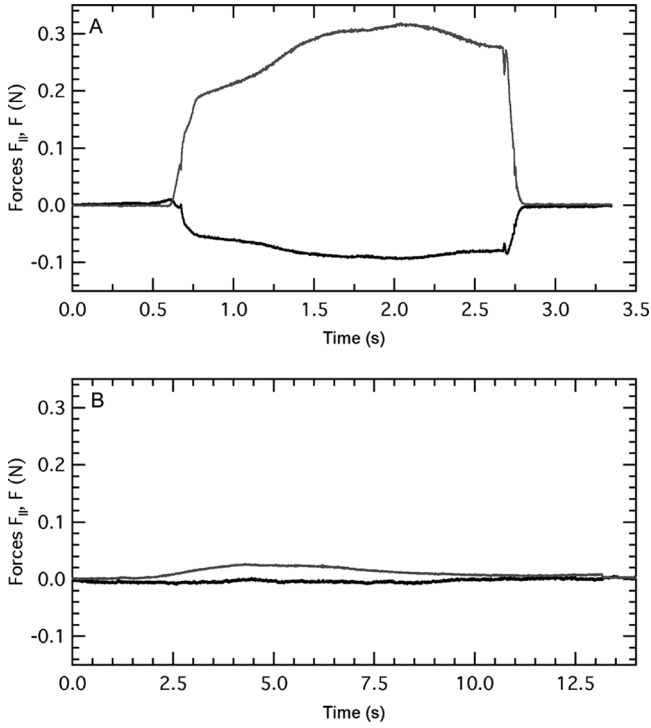

FIGURE 5 Plot of the friction force $F_{||}$ (grey line) and the normal force F (black line) obtained upon shearing a gecko setal array against (A) a glass surface and (B) another setal array. Reprinted with permission from [5]. © 2006, National Academy of Sciences, USA.

fibrillar structures in the tokay gecko. Previous setal array density predictions have used a self-matting criterion [24], which assumes that the minimum inter-pillar spacing is such that setal tips will have sufficient elastic energy stored in their bent state to debond from their neighbor if they had previously been in adhesive contact. Interestingly, self-matting has not been observed in experiments conducted in our lab, suggesting that the self-matting criterion does not apply to the natural gecko adhesive system. Figure 5 shows a typical plot of the friction and adhesion forces obtained when a setal array is sheared against a glass surface (Fig. 5a) over time, compared with a similar experiment performed when a setal array is sheared against another setal array (Fig. 5b). As seen from the results, there is minimal adhesion between setal arrays, consistent with the hypothesis that self-matting between spatula pads is not favorable in the gecko setal array.

We can, however, derive a density criterion based on the bending and crowding properties of the setal array. For the case of tokay geckos, the critical angle of detachment is $\alpha^* = 30^\circ$ [3,20] and sets an *upper* limit on the tilt angle of the setae for adhesion to occur (*i.e.*, for $\theta \geq \alpha^*$, detachment occurs spontaneously). The critical crowding angle $\theta_c = 12.6^\circ$ for the tokay gecko is only expected to be achieved during ground locomotion when the weight of the gecko enhances the preload. During vertical climbing and inverted locomotion, where both adhesion *and* friction are important, the relevant crowding angle to consider is the angle at the first crowding event $\theta_{c,x} = 27.8^\circ$ (*i.e.*, the crowding between nearest neighboring setae). Had the setal density of the tokay been greater (either due to setae of larger radius, r, or smaller setae spacing, s), the crowding angle, $\theta_{c,x}$, would be larger than α^* and detachment would occur spontaneously. The crowding criterion for setal density thus means that, at a minimum, setal crowding must occur *below* the adhesive's critical angle of detachment, α^*. We note that different species of geckos have different critical angles of detachment, α^*, and, furthermore, synthetic dry adhesives might not necessarily have an in-built detachment angle. The above analysis is, therefore, only applicable to the tokay gecko or other gecko species with known detachment angles.

The number density, ρ, of the setae in the Tokay gecko is $\rho = \frac{4}{s^2}$ (since the array consists of four setae within a unit area of dimension, s^2). Substituting the latter relationship for the packing density into Eq. (1) and using the critical detachment angle, α^*, we obtain the crowding criterion as follows:

$$\rho = \left(\frac{2 \sin(\alpha^*)}{d} \right)^2 . \tag{6}$$

For a tokay gecko setal array, Eq. (6) predicts a number density of setae within a unit area of the array of $\sim$14,200 setae/mm^2 (using $\alpha^* = 30^\circ$, $d = 8.4\,\mu$m). This prediction is closer to the actual density of setal arrays of 14,400 setae/mm^2 [25] compared with previous predictions based on self-matting.

The crowding model provides an *upper-bound* (*i.e.*, the maximum number of setae that can be packed per unit area) to the number density of setae based on the detachment angle. The determination of the lower bound of the number density is more complex and is dependent on the friction properties of the material. Although a less dense packing of setae would allow the setae to achieve a smaller tilt angle, thus resulting in stronger adhesion [5,6], one also needs to consider the friction force that plays an implicit role as an anchor, preventing sliding.

Since the friction force is proportional to the contact area (assuming that friction is adhesion-controlled [6,26]), a less dense packing of setae (*i.e.*, fewer setae per area or an overall decrease in real contact area) would result in a lower friction force and allow sliding. Therefore, the optimal design criteria for the geometrical parameters of synthetic dry adhesives inspired by the gecko adhesive system will require a balance between achieving both high adhesion and high friction.

It is also worth noting that the natural tokay gecko setae are curved at the end as seen in the inset of Fig. 2. Although the crowding model does not take the curvature of the setae into consideration, we do not dismiss its importance. As demonstrated by Gravish *et al.* [21], the curvature in the setae acts as a spring that stores elastic energy, which is released during detachment of the setae. The curvature also inherently minimizes the true contact between setae under compression by limiting the contact area to a point contact, thereby minimizing adhesive forces between the setae.

Based on this work, we propose that a synthetic dry adhesive based on the gecko ought to (in addition to having a pad-like end structure mimicking a gecko spatula pad that provides intimate true contact with surfaces [27]) have optimized design parameters including (i) the diameter of the pillars and inter-pillar spacing in order to maximize both adhesion and friction, (ii) the tilt angle of the pillars in order to allow for anisotropic friction and adhesion based on the shearing direction, and (iii) pillar curvature to minimize inter-pillar adhesion.

CONCLUSION

A model based on geometrical considerations of pillars in a square lattice was analyzed to predict the point at which the pillars crowd when subjected to a compressive force. The crowding model predicted that at a critical compression depth of $\Delta z_c = 49\,\mu\text{m}$ the normal stiffness of the adhesive would undergo a dramatic increase, consistent with experimental data, at which point the final tilt angle of the setae would be $\theta_c = 12.6^\circ$ for the setal array of a tokay gecko. The transition of the setae from the uncrowded state to the crowded state does not occur abruptly but instead progresses through a gradual increase of setae becoming crowded upon further compression. In addition, the crowding model was used to derive a criterion to predict the number density of setae within a setal array based on the detachment angle. The predicted value of $14{,}200\,\text{setae}/\text{mm}^2$ is consistent with actual setae density. The latter suggests that, for the case of tokay geckos, the geometrical properties of the pillars including the diameter, d,

and inter-pillar spacing, s, as opposed to the surface properties of the structures, are critical in determining the maximum number density of the setae within the setal array.

ACKNOWLEDGMENT

This work was supported by the Institute for Collaborative Biotechnologies Grant DAAD19-03-D-0004 (JI) from the U.S. Army Research Office, NSF-NIRT 0304730 (K.A), and DCI/NGIA HM1582-05-2022 (K.A & J.I.)

REFERENCES

[1] Ruibal, R. and Ernst, V., *J. Morphol.* **117**, 271–294 (1965).
[2] Williams, E. E. and Peterson, J. A., *Science* **215**, 1509–1511 (1982).
[3] Autumn, K., Liang, Y. A., Hsieh, S. T., Zesch, W., Chan, W. P., Kenny, T. W., Fearing, R., and Full, R. J., *Nature* **405**, 681–685 (2000).
[4] Irschick, D. J., Austin, C. C., Petren, K., Fisher, R. N., Locos, J. B., and Ellers, O., *Biol. J. Linn. Soc.* **59**, 21–35 (1996).
[5] Tian, Y., Pesika, N. S., Zeng, H. B., Rosenberg, K., Zhao, B., McGuiggan, P., Autumn, K., and Israelachvili, J., *PNAS* **103**, 19320–19325 (2006).
[6] Pesika, N. S., Tian, Y., Zhao, B., Rosenberg, K., Zeng, H. B., McGuiggan, P., Autumn, K., and Israelachvili, J., *J. Adhesion* **83**, 383–401 (2007).
[7] Kim, T. W. and Bhushan, B., *J. Adhes. Sci. Technol.* **20**, 1–20 (2007).
[8] Bhushan, B., Peressadko, A. G., and Kim, T. W., *J. Adhes. Sci. Technol.* **20**, 1475–1491 (2006).
[9] Zhao, B., Pesika, N. S., Rosenberg, K., Tian, Y., Zeng, H. B., McGuiggan, P., Autumn K., and Israelachvili, J., *Langmuir* **24**, 1517–1524 (2008).
[10] Autumn, K., Sitti, M., Liang, Y. A., Peattie, A. M., Hansen, W. R., Sponerg, S., Keny, T. W., Fearing, R., Israelachvili, J. N., and Full, R. J., *PNAS* **99**, 12252–12256 (2002).
[11] Autumn, K. and Gravish, N., *Philos. Trans. R. Soc. London* **366**, 1575–1590 (2008).
[12] Del Campo, A. and Arzt, E., *Macromol. Biosci.* **7**, 118–127 (2007).
[13] Qu, L. T., Dai, L. M., Stone, M., Xia, Z. H., and Wang, Z. L., *Science* **322**, 238–242 (2008).
[14] Persson, B. N. J., *MRS Bulletin* **32**, 486–490 (2007).
[15] Takahashi, K., Berengueres, J. O. L., Obata, K. J., and Saito, S., *Int. J. Adhes. Adhes.* **26**, 639–643 (2006).
[16] Huber, G., Gorb, S. N., Hosoda, N., Spolenak, R., and Arzt, E., *Acta Biomaterialia* **3**, 607–610 (2007).
[17] Autumn, K., Majidi, C., Grff, R. E., Dittmore, A., and Fearing, R., *J. Exp. Biol.* **209**, 3558–3568 (2006).
[18] Russell, A. P., *J. Zool.* **176**, 437–476 (1975).
[19] Peattie, A. M., Majidi, C., Corner, A., and Full, R. J., *J. Roy. Soc. Interface* **4**, 1071–1076 (2007).
[20] Autumn, K., Dittmore, A., Santos, D., Spenko, K., and Cutkosky, M., *J. Exp. Biol.* **209**, 3569–3579 (2006).
[21] Gravish, N., Wilkinson, M., and Autumn, K., *J. R. Soc. Interface* **5**, 339–348 (2008).

[22] Russell, A. P., Johnson, M. K., and Delannoy, S. M., *J. Adhes. Sci. Technol.* **21**, 1119–1143.
[23] Boyce, W. E. and Diprima, R.C., *Elementary Differential Equations*, 4th Ed., (John Wiley & Sons, New York, 1986).
[24] Sitti, M. and Fearing, R. S., *J. Adhes. Sci. Technol.* **17**, 1055–1073 (2003).
[25] Autumn, K. and Peattie, A. M., *Integr. Comp. Biol.* **42**, 1081–1090 (2002).
[26] Gao, J. P., Luedtke, W. D., Gourdon, D., Ruths, M., Israelachvili, J. N., and Landman, U., *J. Phys. Chem. B* **108**, 3410–3425 (2004).
[27] Zhao, B., Pesika, N. S., Zeng, H., Wei, Z., Chen, Y., Autumn, K., Turner, K., and Israelachvili, J. *J. Phys. Chem. B* **113**, 3615–3612 (2009).